Separation Science and Technology
Publication details, including instructions for authors and subscription information:
http://www.informaworld.com/smpp/title~content=t713708471

A New Method for the Theoretical Analysis of Electroforced Sedimentation Using Terzaghi-Voigt Combined Model

M. S. Jami[a]; M. Iwata[b]
[a] Faculty of Engineering, Department of Biotechnology Engineering, International Islamic University Malaysia, Kuala Lumpur, Malaysia [b] Department of Chemistry and Biochemistry, Suzuka National College of Technology, Suzuka, Japan

To cite this Article Jami, M. S. and Iwata, M.(2008) 'A New Method for the Theoretical Analysis of Electroforced Sedimentation Using Terzaghi-Voigt Combined Model', Separation Science and Technology, 43: 5, 979 — 995

To link to this Article: DOI: 10.1080/01496390801888078

URL: http://dx.doi.org/10.1080/01496390801888078

Separation Science and Technology, 43: 979–995, 2008
Copyright © Taylor & Francis Group, LLC
ISSN 0149-6395 print/1520-5754 online
DOI: 10.1080/01496390801888078

A New Method for the Theoretical Analysis of Electroforced Sedimentation Using Terzaghi-Voigt Combined Model

M. S. Jami[1] **and M. Iwata**[2]

[1]Faculty of Engineering, Department of Biotechnology Engineering,
International Islamic University Malaysia, Kuala Lumpur, Malaysia
[2]Department of Chemistry and Biochemistry, Suzuka National College of Technology, Suzuka, Japan

Abstract: In this article a new method for the theoretical analysis of electroforced sedimentation (EFS) by use of the Terzaghi-Voigt combined model is presented. Zinc oxide and a mixture of zinc oxide and KC-flock are used as experimental materials. Both the electro-osmotic pressure gradient E_{pg} and the modified consolidation coefficient C_e of the materials are assumed to be constant. The analytical solution can explain the solid compressive pressure distribution with time and position. The progress of electroforced sedeimentation can be represented by an average consolidation ratio U_c as in mechanical expression. Variations of the effectiveness of EFS with the percentage of KC-flock in the mixture, electric current density, and total solid volume per unit cross-sectional area are investigated. EFS is best applied for materials with permanent charge.

Keywords: Electro-osmosis, sedimentation, solid-liquid separation, creep deformation

INTRODUCTION

Sedimentation is an important tool for solid–liquid separation broadly utilized in various process industries. It is a convenient and inexpensive method of

Received 16 August 2007, Accepted 9 December 2007

Address correspondence to M. S. Jami, Faculty of Engineering, Department of Biotechnology Engineering, International Islamic University Malaysia, P. O. Box 10, 50728, Kuala Lumpur, Malaysia. Tel.: 60-3-6196-5466; Fax: 60-3-6196-4442; E-mail: saedi@iiu.edu.my

separating solids from liquids. However, sedimentation under only the gravitational field is time-consuming. Application of electric field to enhance the separation, is one of the techniques studied by various researchers. The positive effect of applying electric field to enhance the separation has been known for several decades. However, the theory explaining the electroforced sedimentation (EFS) has not been successfully developed. There is a desire to better understand EFS due to number of current and potential applications.

In elecroforced sedimentation, the separation of liquid from a solid-liquid mixture is achieved between two electrodes. Its principal use would be in reducing the water content in environmental sludge and biosolids, thereby reducing the volumes to be disposed through landfills, incineration, or other means. In EFS with a moderate electric field strength, the moisture of a solid-liquid mixture remains unchanged at the surface of the sediment, while it decreases drastically near the bottom of the sedimentation column. This fact is widely known; to date however, due to paucity of analytical methods, it has not been successfully explained.

Electro-osmosis refers to the motion of liquid induced by an applied electric field. The application of an electric field to a solid-liquid mixture causes the ions in the double layer to move towards one electrode or the other. Since ions are mostly of one sign, their motion gives rise to a body force on the liquid in the double layer, and it is this body force, which sets the liquid in motion (1). Various research results have been reported concerning the electrokinetic phenomena. Shirato et al. developed a basic mathematical method for analyzing electroforced settling behavior (2). Yi and Iwata analyzed the EFS of highly concentrated clay slurry in consolidation region (3). Iwata et al. developed a simplified theoretical model for electro-osmotic dewatering to predict the compressive pressure distribution of solid-liquid systems across the cake as a function of time and position (4). In another report, an analytical solution of the basic differential equation that describes the progress of an electro-osmotic dewatering was presented (5).

The main goal of this research work is to analytically solve the basic differential equation that controls the progress of EFS by considering the creep deformation of the material. The equation is tested and compared to the experimental data. Constant-current EFS is analyzed by use of the Terzaghi-Voigt combined model by assuming that the electroosmotic properties of the materials are constant. EFS experiments under constant electric current density of zinc oxide and mixture of zinc oxide and KC-flock suspended in aqueous media are carried out and comparison is made between the experimental results and model predictions. Settling rates are measured by monitoring the progress of sedimentation continuously using a video camera. The effects of percentage of KC-flock in the mixture, current density, and the total solid volume per unit cross-sectional area are studied. EFS parameters of the material such as the modified consolidation coefficient C_e and the ratio of the creep deformation to the total deformation B, are analyzed. Furthermore, a method is developed to determine the effectiveness of EFS using the theoretical equation.

EXPERIMENTAL

A sedimentation column (Fig. 1) 45 cm high and 4 cm internal diameter made of acryl was used. The electrodes, both made of stainless steel, are placed in parallel at the top and the bottom of the column. During EFS, the bottom electrode is connected to the negative terminal of the power supply as the cathode, and the top electrode is connected to the positive terminal as the anode. Hence, zinc oxide particles with positive charges will be expelled from the top of the sedimentation column and move towards the bottom (cathode), thus, inducing enhanced sedimentation.

As experimental materials, zinc oxide (Nacalai Tesque, Inc.) or mixture of zinc oxide and KC-flock (Nippon Paper Chemicals Co., Ltd.) were used. KC-flock is finely powdered cellulose manufactured from wood pulp. The zinc oxide has median diameter of 0.849 μm and density of $5420\,\mathrm{kg/m^3}$ while the corresponding values of median diameter and density for the KC-flock are 31.7 μm and $1610\,\mathrm{kg/m^3}$, respectively. The density of the mixture was evaluated by using the true density of the individual component and considering its proportion in the mixture. The slurry used in the experiments was prepared by mixing a predetermined quantity of dry solid (zinc oxide alone or mixed with KC-flock) and deionized water to form a suspension of known total solid volume per unit cross-sectional area. The slurry was then poured into the sedimentation column and left until gravitational sedimentation was completed and equilibrium height was achieved. The electric field was provided by a dc power supply with a capacity of 350 V and 0.2 A (KIKUSUI PMC350-0.2A) through the top anode and bottom cathode under constant-current condition. As settling progresses, the change in height of sediment was visually monitored continuously using a video camera and

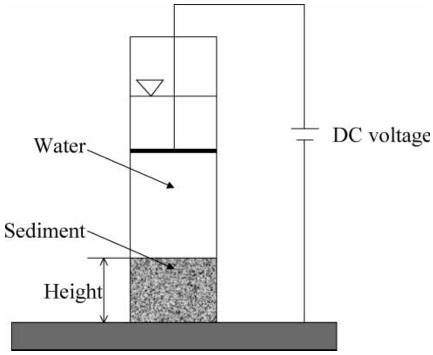

Figure 1. Schematic diagram of experimental apparatus.

finally the solid concentrations in the sedimentation column were measured. When the height became constant, the material was sliced and dried in the oven to obtain the final moisture distribution. Experiments were conducted under various KC-flock composition in the mixture, current densities and total solid volume per unit cross-sectional area.

THEORY

Basic Differential Equation

Kobayashi et al. (6) solved the Navier-Stokes equation to describe an electro-osmotic flow through a capillary tube, taking into account the applied electric field strength and the electric field strength in the electric double layer caused by the contact potential difference. They extended the result to describe an electro-osmotic flow through porous media in much the same way as in the derivation of the Kozeny-Carman equation (7). The apparent liquid velocity q through the porous material is defined by the flow rate per unit cross-sectional area of the material and represented by (8)

$$q = \frac{\varepsilon^3}{kS_0^2(1-\varepsilon)^2\mu}\left(\rho_e E - \frac{dp_L}{dx}\right) \tag{1}$$

where k is the Kozeny constant; ε and S_0, respectively the porosity and specific surface of the material; μ, the viscosity of the liquid; ρ_e, the volumetric charge density of the liquid; and p_L, the liquid pressure. x and E in Eq. (1) are the spatial coordinate and the electric field strength in the direction of material thickness, respectively. The first term of the right-hand side of Eq. (1) represents an electro-osmotic flow in a porous material, while the second term shows a pressure flow in the material, both including the tortuousity and size of flow path. If $E = 0$, then Eq. (1) is reduced to the Kozeny-Carman equation which represents the apparent flow rate through a porous material under a liquid pressure gradient. Kobayashi et al. examined Eq. (1) by use of incompressible sintered glass beads.

As EFS progresses, the height of the material in the sedimentation column decreases. In the analysis of such processes, it is definitely more convenient and more accurate to use the moving material coordinate ω instead of the fixed spatial coordinate x, because not only the liquid but also solid particles move in sedimentation (9). Here ω denotes the net solid volume per unit cross-sectional area extending from the bottom of the sedimentation column up to an arbitrary position in the material. $\omega = 0$ at the lower electrode and $\omega = \omega_0$ at the surface of the sediment; $d\omega = (1-\varepsilon)dx$. In order to maintain the electric neutrality, the charges on the solid are countered by opposite charges in the liquid. Hence, the charge densities on the surface of the solid and in the liquid can be related as follows

$$\sigma_s(1-\varepsilon) = \rho_e\varepsilon \tag{2}$$

where σ_s is the effective charge on solid surface per unit volume of solids. Rearranging Eq. (1) using Ohm's Law ($E = i\rho_E$ where i is the electric current density and ρ_E is the specific electric resistance of the material), and combining it with Eq. (2) after replacing x with ω yield

$$q = \frac{1}{\mu\alpha\rho_s}\left(\frac{\sigma_s i\rho_E}{\varepsilon} - \frac{\partial p_L}{\partial\omega}\right) \tag{3}$$

where ρ_s denotes the true density of solids. α is the specific hydrodynamic resistance defined by

$$\alpha = \frac{kS_0^2(1-\varepsilon)}{\rho_s\varepsilon^3} \tag{4}$$

In the conventional Helmholtz-Smoluchowski equation, the apparent liquid velocity can be written as

$$q = \frac{Di\zeta\rho_E\varepsilon}{\mu} \tag{5}$$

Here D is the dielectric constant and ζ is the zeta potential. Unlike Eq. (3), this equation does not take into account the size and shape of the capillary as well as the tortuosity of the flow path. Hence we started our analysis with Eq. (3) because it is definitely appropriate to consider the tortuousity and size of flow path not only in the case of pressure flow, but also during the analysis of electro-osmotic flow in the porous material.

To discuss the internal mechanism of electroforced sedimentation of compressible materials, the relation between liquid pressure p_L and solid compressive pressure p_s is essential. From the balance of forces acting respectively on the solids and the liquid over the portion dω, the following equation can be obtained (3).

$$-\frac{\partial p_L}{\partial\omega} = (\rho_s - \rho)g + \frac{\partial p_s}{\partial\omega} \tag{6}$$

Mass balance of fluid with respect to a volume element dω yields

$$-\frac{\partial q}{\partial\omega} = \frac{\partial e}{\partial\theta} \tag{7}$$

where e is the local void ratio ($e = \varepsilon/(1-\varepsilon)$).

Using Eq. (6), one can rewrite Eq. (3) as follows.

$$q = \frac{1}{\mu\alpha\rho_s}\left\{\frac{\sigma_s i\rho_E}{\varepsilon} + \frac{\partial p_s}{\partial\omega} + (\rho_s - \rho)g\right\} \tag{8}$$

The first term of the right hand side of Eq. (8) represents an electro-osmotic flow while the remaining terms show pressure flow, all including the tortuousity and size of the flow path.

Combining Eqs. (7) and (8) we have

$$\frac{\partial e}{\partial \theta} = -\frac{\partial q}{\partial \omega} = -\frac{\partial}{\partial \omega}\left[\frac{1}{\mu \alpha \rho_{\mathrm{s}}}\left\{\frac{\sigma_{\mathrm{s}} i \rho_{\mathrm{E}}}{\varepsilon} + \frac{\partial p_{\mathrm{s}}}{\partial \omega} + (\rho_{\mathrm{s}} - \rho) g\right\}\right] \tag{9}$$

From Eq. (9), EFS can be recognized as a kind of consolidation, since it accompanies the increase of solid compressive pressure in the material.

As in mechanical consolidation, the variation of e will be caused by both the change in local compressive pressure p_{s} and the simultaneous effect of creep of solids; e is not a single-valued function of p_{s}, but is a function of both p_{s} and time θ. On the assumption that the mechanical property of the solid network is expressed by the Terzaghi-Voigt combined model shown in Fig. 2, the left hand side of Eq. (9) can be expressed by

$$\left(\frac{\partial e}{\partial \theta}\right)_{\omega} = \left(\frac{\partial e}{\partial p_{\mathrm{s}}}\right)_{\theta}\left(\frac{\partial p_{\mathrm{s}}}{\partial \theta}\right)_{\omega} + \left(\frac{\partial e}{\partial \theta}\right)_{\mathrm{p_s}} \tag{10}$$

The first term on the right-hand side of Eq. (10) indicates the change in e due to the primary consolidation and depends only upon the change in p_{s}.

$$\left(\frac{\partial e}{\partial p_{\mathrm{s}}}\right)_{\theta} = -\frac{1+e}{E_1} \equiv -a_{\mathrm{E}} \tag{11}$$

where E_1 is the elastic coefficient of the spring of the Terzaghi element. The second term of Eq. (10) is that of creep deformation. The term can be

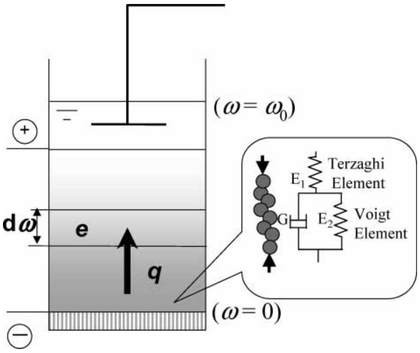

Figure 2. Terzaghi-Voigt combined model.

represented by (12)

$$\left(\frac{\partial e}{\partial \theta}\right)_{\mathrm{p_s}} = -\frac{\partial}{\partial \theta}\left[a_c \eta \int_0^{\theta} \{p_s(\omega, \tau) - p_s(\omega, 0)\}\exp\{-\eta(\theta - \tau)\}d\tau\right] \tag{12}$$

where $a_c = (1 + e)/E_2$; $\eta = E_2/G$; E_2 and G are the elastic coefficient of the spring and the viscosity of the dashpot of the Voigt element, respectively. We define the modified consolidation coefficient (9), C_e, by Eq. (13) as in mechanical expression and the electro-osmotic pressure gradient E_{pg} which is the driving force of EFS and is defined by Eq. (14).

$$C_e = \frac{1}{\mu\alpha\rho_s(-de/dp_s)_{\theta}} \tag{13}$$

$$E_{pg} = \frac{\sigma_s i \rho_E}{\varepsilon} \tag{14}$$

C_e and E_{pg} are functions of time and position. To obtain the following differential equation and its analytical solution, the average values of both C_e and E_{pg} are assumed to be constant. Such a technique has also been used in the analysis of mechanical expression. The analytical solution helps to understand the effect of each parameter on sedimentation, as described later. Assuming C_e and E_{pg} are constant and substituting Eqs. (10), (11), (12), and (13) into Eq. (9), we obtain the basic equation, which controls the progress of EFS.

$$\frac{\partial p_s}{\partial \theta} + \beta\frac{\partial}{\partial \theta}\left[\eta \int_0^{\theta} [p_s(\omega, \tau) - p_s(\omega, 0)]\exp\{-\eta(\theta - \tau)\}d\tau\right] = C_e\frac{\partial^2 p_s}{\partial \omega^2} \tag{15}$$

Here $\beta = a_c/a_E$.

The initial and boundary conditions for Eq. (15) under constant electric current are

$$p_s = p_0 + (\omega_0 - \omega)(\rho_s - \rho)g \quad \text{at } \theta = 0 \tag{16}$$

$$p_s = p_0 \quad \text{at } \omega = \omega_0 \text{ (surface of sediment)} \tag{17}$$

$$\frac{\partial p_s}{\partial \omega} = -E_{pg} - (\rho_s - \rho)g \quad \text{at } \omega = 0 \text{ (no liquid flow at the bottom)} \tag{18}$$

Eq. (18) is the impermeable bottom condition, i.e. $q = 0$.

The solution of Eq. (15) is given by the following equation, representing the solid compressive pressure distribution in the material as a function of time and position.

$$p_s(\omega,\theta) = [E_{pg} + (\rho_s - \rho)g](\omega_0 - \omega) + p_0 - \sum_{n=1}^{\infty}\left[\frac{8\omega_0 E_{pg}(-1)^{n-1}\sin\{((2n-1)\pi/2)(1-(\omega/\omega_0))\}}{(2n-1)^2\pi^2} \times \exp\left\{-\frac{(2n-1)^2\pi^2}{4}\frac{C_e}{\omega_0^2}\theta\right\}\right] \tag{19}$$

The total decrease in material thickness can be calculated from the equation

$$H_1 - H = \int_0^{\omega_0}(e_1 - e)d\omega \tag{20}$$

where e_1 and e are the initial and instantaneous void ratio distribution of the material, respectively. Similarly, H_1 and H are the initial and instantaneous height of the sediment, respectively.

Integration of Eq. (10) with respect to θ gives the change in local void ratio during time θ.

$$e_1 - e = a_E\int_0^{\theta}\frac{\partial p_s}{\partial\theta}d\theta + a_c\eta\int_0^{\theta}\{p_s(\omega,\tau) - p_s(\omega,0)\}\exp\{-\eta(\theta-\tau)\}d\tau \tag{21}$$

Substituting Eq. (19) into Eq. (21) and integrating with respect to ω, we obtain the following equation of the average consolidation ratio U_c, which is a measure of the progress of EFS.

$$U_c = \frac{H_1 - H}{H_1 - H_\infty} = (1-B)\left[1 - \frac{32}{\pi^3}\sum_{n=1}^{\infty}\frac{(-1)^{n-1}}{(2n-1)^3} \times \exp\left\{-\frac{(2n-1)^2\pi^2}{4}\frac{C_e}{\omega_0^2}\theta\right\}\right] + B[1 - \exp(-\eta\theta)] \tag{22}$$

where H_∞ is the final height of the material. B is an empirical constant defined by $B = a_c/(a_c + a_E)$ and represents the ratio of the creep deformation to the total deformation. U_c is zero at the beginning and becomes unity at infinite EFS time.

Determination of the Creep Constants, B and η

If $\pi^2 C_e/(4\omega_o^2) > \eta$, then Eq. (22) becomes approximately the following equation when $\theta \gg 0$.

$$U_c \approx 1 - B\exp(-\eta\theta) \tag{23}$$

In consideration of this equation, the values of both B and η can be graphically determined from the later stage of the experimental results plotted as $\ln(1 - U_c)$ vs. θ.

Determination of the Modified Consolidation Coefficient C_e

For determining the experimental C_e-value in Eq. (22), a fitting method can be used. Eq. (22) can be rearranged as

$$U_{c\cdot corr} = \frac{U_c - B[1 - \exp(-\eta\theta)]}{1 - B} = 1 - \frac{32}{\pi^3}\sum_{n=1}^{\infty}\frac{(-1)^{n-1}}{(2n-1)^3} \times \exp\left\{-\frac{(2n-1)^2\pi^2}{4}T_c\right\} \tag{24}$$

T_c is the consolidation time factor defined by

$$T_c = \frac{C_e\theta}{\omega_0^2} \tag{25}$$

In Eq. (24), $U_{c\cdot corr} = 0.700$ when $T_c = 0.501$. Accordingly, an empirical C_e-value can be determined from the following equation

$$C_e = 0.501\frac{\omega_0^2}{\theta_{70}} \tag{26}$$

where θ_{70} is the experimental time required for attaining 70% of $U_{c\cdot corr}$.

Determination of the Electro-Osmotic Pressure Gradient E_{pg}

The total decrease in material thickness can be calculated from the equation

$$H_1 - H_\infty = \int_0^{\omega_0}(e_1 - e_\infty)\mathrm{d}\omega \tag{27}$$

where e_∞ is the final void ratio distribution of the material.

Table 1. Compression data for zinc oxide

Pressure range of p_s [Pa]	E_0 [−]	C_c [−]
$p_s < 480$	33.1	2.60
$480 < p_s < 30000$	35.6	3.00

A local void ratio e is a function of local solid compressive pressure p_s as expressed by the following Terzaghi-Peck equation (13).

$$e = E_0 - C_c \ln p_s \tag{28}$$

where E_0 and C_c are constants and can be obtained from the compression-permeability tests. Experimentally determined E_0 and C_c values with the corresponding pressure ranges for zinc oxide are given in Table 1.

Substituting $\theta = \infty$ in Eq. (19), we obtain the final solid compressive pressure distribution as follows.

$$p_s(\omega, \infty) = \left[E_{pg} + (\rho_s - \rho)g\right](\omega_0 - \omega) + p_0 \tag{29}$$

Combining Eqs. (27)–(29), we obtain

$$H_1 - H_\infty = \int_0^{\omega_0} C_c \ln \frac{p_0 + \{E_{pg} + (\rho_s - \rho)g\}(\omega_0 - \omega)}{p_0 + (\rho_s - \rho)g(\omega_0 - \omega)} \mathrm{d}\omega \tag{30}$$

Thus, the electro-osmotic pressure gradient E_{pg} can be determined from Eq. (30), using empirical value of $H_1 - H_\infty$.

Definition of the Effectiveness of EFS η_{eff}

We define the effectiveness of EFS as

$$\eta_{eff} = \frac{e_1 - e_{av,\infty}}{e_1} = \frac{C_c}{e_1} \int_0^1 \ln \frac{p_0 + \{E_{pg} + (\rho_s - \rho)g\}\omega_0(1 - \omega/\omega_0)}{p_0 + (\rho_s - \rho)g\omega_0(1 - \omega/\omega_0)} d\left(\frac{\omega}{\omega_0}\right) \tag{31}$$

Thus, the effectiveness depends on the compression property of the material C_c, the total solid volume per unit cross-sectional area ω_0, and the electro-osmotic pressure gradient E_{pg}, which in turn is a function of current density i and the specific electric resistance of the material.

RESULTS AND DISCUSSION

Figure 3 shows the time course of changes in solid compressive pressure p_s, calculated from Eq. (19), while Figure 4 shows the distribution of void ratio e, obtained by combining Eqs. (19) and (28). In the figures, ω/ω_0 represents an arbitrary position along the height of the sediment ($\omega/\omega_0 = 0$ at the bottom, and $\omega/\omega_0 = 1$ at the top of the sediment). At the start of operation ($\theta = 0$ and hence $U_c = 0$), there exists an initial p_s-distribution as indicated by Eq. (16) and consequently it results in an e-distribution across the sediment due to the natural sedimentation under gravity. After the application of electric field, further decrease of void ratio e starts from the layer nearest the lower electrode ($\omega/\omega_0 = 0$). Since $q = 0$ at the bottom of the sediment, the liquid pressure gradient $\partial p_L/\partial\omega$ should be positive ($=E_{pg}$) from Eq. (3). The positive $\partial p_L/\partial\omega$ is offset by the negative $\partial p_s/\partial\omega$ arising from the force balance (Eq. (6)), resulting in the increase in solid compressive pressure p_s near the bottom electrode. This increase in p_s leads to a reduction of the local void ratio e. Thus, as mentioned in the theory section, electroforced sedimentation can be recognized as a kind of consolidation, since it accompanies the increase of solid compressive pressure in the material. At the equilibrium state, $\partial e/\partial\theta$ in Eq. (9) should be zero, i.e., the electro-osmotic flow and the pressure flow cancel each other out in all layers of the sediment. It can be observed that the shape of the curve at $U_c = 0.1$ in Fig. 4 differs from the rest of the curves. This could be due to the diminishing effect of p_s on the local void ratio as U_c decreases, which itself depends on the compression data of zinc oxide.

Figure 5 shows the void ratio distribution of the final cake for the case of experiment with only zinc oxide. The experimental void ratio is obtained by slicing the final sediment and drying in the oven. The solid line in the figure

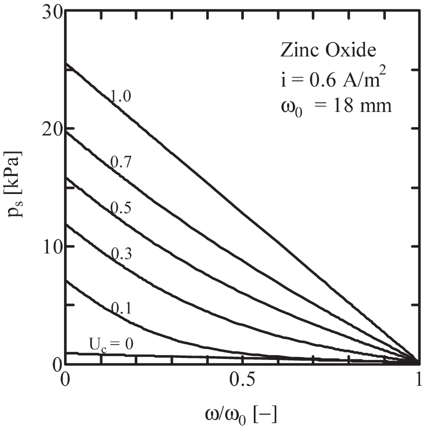

Figure 3. Theoretically calculated solid compressive pressure distribution.

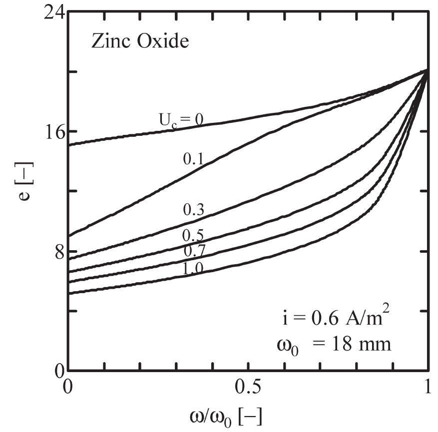

Figure 4. Theoretically calculated void ratio distribution.

represents the theoretical prediction calculated from Eqs. (28) and (29). The theory agrees well with the experiment.

Figure 6 represents the time course of U_c during EFS of mixture of zinc oxide and KC-flock. Both lines represent the calculated results obtained by using Eq. (22). When $B = 0.268$ in Eq. (22), i.e., when the creep deformation of the material is taken into consideration, there is a good agreement between calculated and experimentally obtained values. The effect of creep deformation becomes apparent when zinc oxide is mixed with KC-flock (Fig. 7). For experiments with only zinc oxide, the creep ratio B is zero, i.e., the primary consolidation is dominant and hence the creep deformation does not exist. For mixture of zinc oxide and KC-flock, the Terzaghi model is not sufficient to express the mechanical properties of the particles. As the

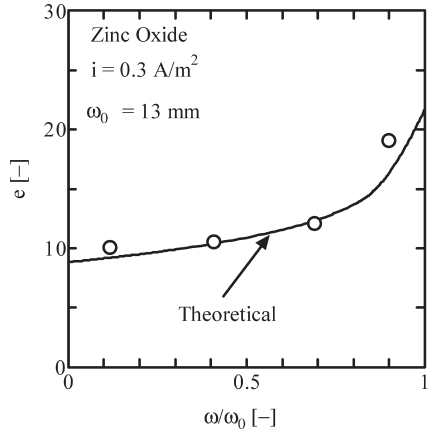

Figure 5. Theoretical and experimental final void ratio distributions.

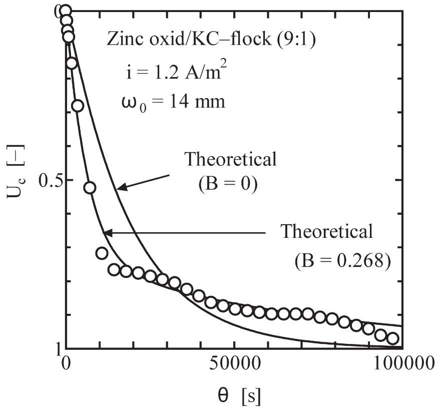

Figure 6. Progress of EFS with electroforced sedimentation time.

composition of the KC-flock in the mixture becomes larger, the secondary consolidation dominates and the value of *B* increases.

Figure 8 depicts the effect of current density *i* on the effectiveness of EFS, expressed as the difference between average void ratios of the material before and after EFS. As can be seen in the figures, higher current density is more effective. Figure 9 illustrates the effect of current density *i* on the electro-osmotic pressure gradient E_{pg}, which is the driving force for the EFS. It can be seen that E_{pg} increases with an electric current density *i*; a larger E_{pg} results in a higher solid compressive pressure distribution in the material, as is clear from Eq. (19). Higher current density gives rise to higher E_{pg}

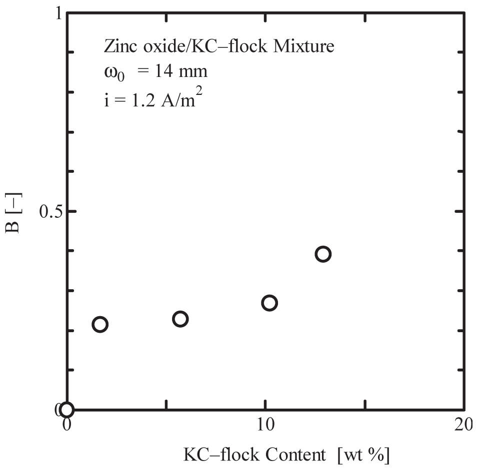

Figure 7. Variation of the creep ratio with KC-flock composition.

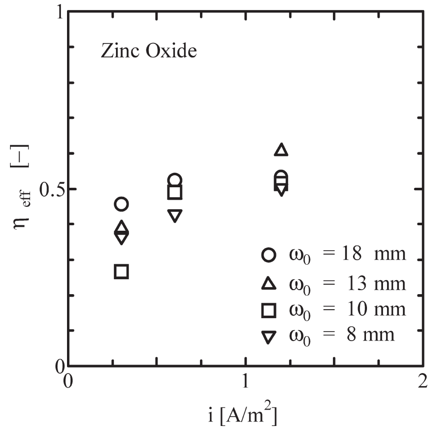

Figure 8. Effect of current density on the effectiveness of EFS for various total volume per unit cross sectional area.

(Eq. (14)) and this in turn brings about higher p_s (Eq. (19)), which results in improved sedimentation (Fig. 8).

Figure 10 shows the effectiveness of EFS against the composition of KC-flock in the mixture. For the experimental range covered in this study, the effectiveness decreases as the percentage of KC-flock in the mixture becomes higher. Since KC-flock particles have almost no charge on their surface, sedimentation is not effective as KC-flock being predominant in the mixture. However, further experiments should be carried out to investigate the trend with higher content of the KC-flock.

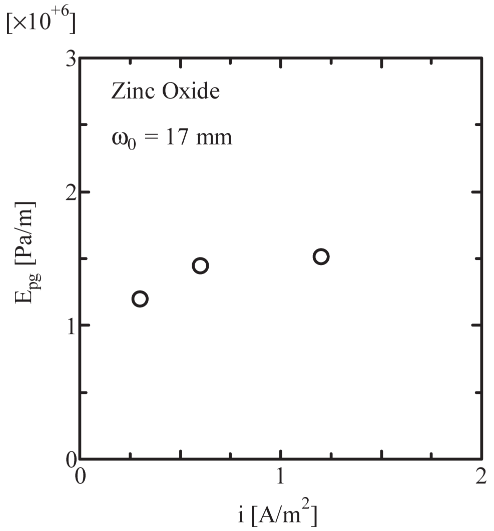

Figure 9. Relationship between electro-osmotic pressure gradient and current density.

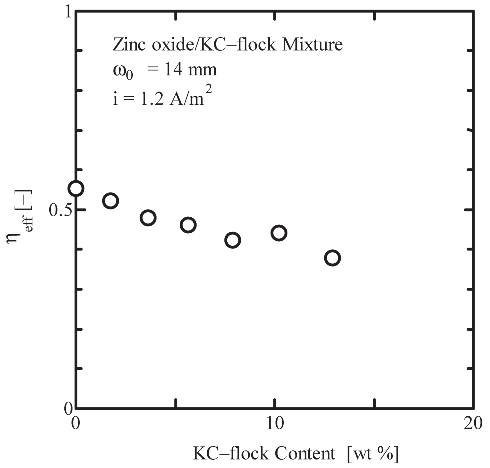

Figure 10. Effectiveness of EFS as a function of KC-flock composition.

Figure 11 displays the relationship of empirical values of the modified consolidation coefficient C_e with the composition of KC-flock. The empirical values of C_e are determined using the fitting method as explained in the theory section. The value of C_e becomes smaller as the composition of KC-flock increases. The modified consolidation coefficient involves information about the deformation process of the sediment under electric field. The dimension of C_e is the same as that of the diffusion coefficient. Hence the consolidation process of the material can be recognized as the diffusion

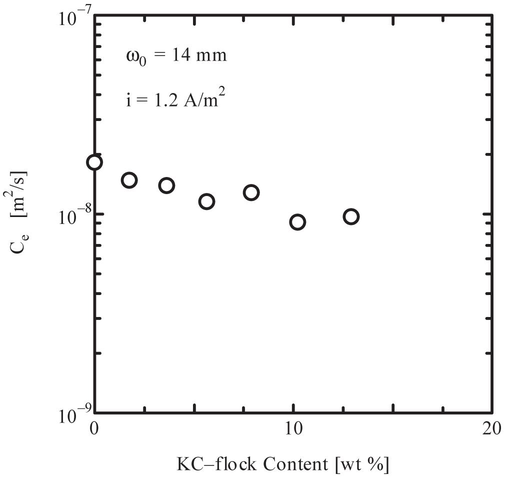

Figure 11. Variation of the modified consolidation coefficient with KC-flock composition.

process of the compact layer. A smaller C_e leads to a smaller sedimentation rate, as is obvious from Eqs. (19) and (22).

CONCLUSIONS

The basic differential equation for a constant current EFS was solved under the assumption that the electro-osmotic property does not change during the process. A decrease in moisture of the sediment begins at the bottom electrode. The analytical solution can explain the time course of changes in a solid compressive pressure distribution and distribution of the void ratio. The progress of EFS can be represented by an average consolidation ratio U_c as in mechanical expression. The agreement between calculated and experimental U_c is satisfactory when the creep deformation of the material is considered for the mixture of zinc oxide and KC-flock. The effectiveness of EFS can be expressed by the relative difference of void ratios of the sediment before and after EFS. The effectiveness of EFS is described as a function of current density i and total solid volume per unit cross sectional area ω_0. The effectiveness of EFS decreases, as the percentage of KC-flock in the mixture gets higher. This is due to the fact that KC-flock particles have very little charge. Hence, it can be concluded that EFS, as the main solid-liquid separation process, is best applied for materials with permanent charge.

ACKNOWLEDGMENTS

This work was supported by grant-in-aid from Japan Society for the Promotion of Science (grant number 17-05155). The authors would like to acknowledge the financial support with sincere gratitude.

REFERENCES

1. Iwata, M. (1995) Electroosmotic dewatering. In *Electric Field Applications in Chromatography, Industrial and Chemical Processes*; Tsuda, T. (ed.); VCH, 133–151.
2. Shirato, M., Aragaki, T., Manabe, A., and Takeuchi, N. (1979) Electroforced sedimentation of thick clay suspensions in consolidation region. *Chemical Engineering Progress*, 25: 855–863.
3. Yi, W.D. and Iwata, M. (1995) Analysis of an electroforced sedimentation of highly concentrated clay slurry in consolidation region. *Korean Journal of Chemical Engineering*, 12: 576–581.
4. Iwata, M., Igami, H., Murase, T., and Yoshida, H. (1991) Analysis of electro-osmotic dewatering. *Journal of Chemical Engineering Japan*, 24: 45–50.
5. Iwata, M., Sato, M., and Nagase, H. (2004) Analysis of constant-current electro-osmotic dewatering. *Kagakukogaku Ronbunshu*, 5: 626–632.

6. Kobayashi, K., Iwata, M., Hosoda, Y., and Yukawa, H. (1979) Fundamental study of electro-osmotic flow through perforated membrane. *Journal of Chemical Engineering Japan*, 12: 466–471.
7. Carman, P.C. (1937) Fluid flow through granular beds. *Transactions of the Institution of Chemical Engineering*, 15: 150–166.
8. Kobayashi, K., Hakoda, M., Hosoda, Y., Iwata, M., and Yukawa, H. (1979) Electro-osmotic flow through particle beds and electro-osmotic pressure distribution. *Journal of Chemical Engineering Japan*, 12: 492–494.
9. Shirato, M., Murase, T., Tokunaga, H., and Yamada, O. (1974) Calculations of consolidation period in expression operations. *Journal of Chemical Engineering Japan*, 7: 229–231.
10. Shirato, M., Murase, T., Kato, H., and Fukaya, S. (1967) Studies on expression of slurries under constant pressure. *Kagaku Kogaku*, 31: 1125–1131.
11. Iwata, M., Jami, M.S., and Sato, M. (2007) Analysis of constant-current electro-osmotic dewatering of various solid-liquid systems by considering the creep deformation. *Separation and Purification Technology*, 58: 274–281.
12. Gibson, R.E. and Lo, K.Y. (1961) *A Theory of Consolidation for Soils Exhibiting Secondary Compression*; Norwegian Geotechnical Institute Publication No. 41 pp. 1–16.
13. Taylor, D.W. (1959) *Fundamentals of Soil Mechanics*; Modern Asia (ed.); Charles E. Tuttle: Tokyo.